Adaptive Synchronization Control of a Planar Parallel Manipulator

Lu Ren, James K. Mills, *Member, IEEE* and Dong Sun, *Member, IEEE*

***Abstract*—In this paper, a new control algorithm for a planar parallel robotic manipulator with three degrees-of-freedom (DOF) and parametric uncertainties has been developed. From its mechanical structure, the studied planar parallel manipulator is categorized as a P-R-R type and can be treated as comprised of three constrained sub-manipulators. Key to the successful trajectory tracking control of the P-R-R manipulator is the motion of the sub-manipulators: each sub-manipulator should be controlled to follow its pre-determined trajectory while coordinating motions with the other sub-manipulators. The control algorithm developed employs the above idea and incorporates synchronization technology with the adaptive control architecture by feeding back position, velocity errors of the actuated joints and a newly defined synchronization error. Employment of the synchronization error, verified by simulations, substantially reduces the pose error of the end-effector of the P-R-R manipulator during trajectory tracking. From theoretical analysis, the proposed control algorithm is shown to guarantee the convergence of tracking errors and the synchronization error at the same time. Finally, simulation results demonstrate that the proposed controller can achieve excellent trajectory tracking performance.**

I. INTRODUCTION

As a result of high rigidity, high accuracy and high payload, parallel robotic manipulators have received significant attention and have been applied in various industrial areas [1][2] since the 1980's. In order to execute different tasks, parallel robotic manipulators with different structures have been proposed, such as the Pierrot's manipulator [3], the Hexaglide manipulator [4], the biped manipulator [5] and so on. Recently, with the discovery of the potential of integrating parallel manipulators with reduced number of DOF, planar parallel manipulators have been applied to perform electronic component placement tasks especially in the electronic industry [6]. These mechanisms have simple mechanical structure, high speed performance and low manufacturing and operation cost. A planar parallel manipulator usually consists of several closed-loop chains and one moving platform. In terms of the joints used in one closed-loop chain, planar parallel manipulator are categorized as R-R-R type, R-P-R type, P-R-R type, etc., where P and R mean prismatic and revolute joints, respectively. Since the actuators are fixed on the base and three closed-loop chains support the moving platform, planar parallel manipulators have large stiffness and low inertia that results in high positioning accuracy and fast movement [7].

In this paper, we study a P-R-R type planar parallel manipulator with three DOF and develop a controller to achieve its trajectory tracking. Trajectory tracking is controlling manipulator end-effector move along a path in space with a particular orientation, which is indispensable for robotic manipulator operation. Studying the literature on trajectory control of robotic manipulators reveals that numerous control methods have been proposed, for example, robust control [8], adaptive control [9], neural network [10], etc. However, considering the cost of control energy and the system characteristics: parametric uncertainties due to unknown payloads; performance requirements of high speed and high accuracy, it is not suitable to use these control methods, directly. Here, a control algorithm termed as adaptive synchronization (A-S) control has been developed. A-S control is an adaptive-based control, which incorporates synchronization control into an adaptive control structure. Although synchronization control has been employed on coordination of multiple robots [11], it is reasonable to employ this control method on the P-R-R manipulator due to its mechanical architecture and motion characteristic. From its mechanical architecture, the P-R-R manipulator can be treated as comprised of three constrained sub-manipulators. The end-effectors of the sub-manipulators are all connected to a common payload of the P-R-R manipulator. As a result, the three sub-manipulators move synchronously. Therefore, control of the pose of the P-R-R manipulator end-effector may be achieved by controlling all sub-manipulators simultaneously. Key to the success of

Manuscript received September 22, 2003. This work is supported in part by NSERC.

Lu Ren is a Ph.D. candidate studying in Laboratory for Nonlinear Systems Control, Department of Mechanical Engineering, University of Toronto, Toronto, ON M5S3G8 Canada. (phone: 416-978-0640; fax: 416-978-0640; email: ren@mie.utoronto.ca).

James K. Mills is a Professor in Department of Mechanical Engineering, University of Toronto, Toronto, ON M5S3G8 Canada. (e-mail: mills@mie.utoronto.ca).

Dong Sun is a Professor in Department of Manufacturing Engineering and Engineering Management, City University of Hong Kong, Hong Kong, P.R. China. (e-mail: medsun@cityu.edu.hk).

synchronization control of the P-R-R manipulator is the motion of the three sub-manipulators: each sub-manipulator should be controlled to follow its pre-determined trajectory while coordinating motions with the other sub-manipulators. In synchronization control, besides the position errors and the velocity errors of the actuated joints in the sub-manipulators, a newly defined synchronization error is also fed back. The synchronization error is calculated by using position and velocity errors of all actuated joints. Furthermore, a bounded-gain-forgetting (BGF) adaptation law [12] is employed to minimize the effect of parametric uncertainties in the dynamic model of the P-R-R manipulator and estimate their true values. Theoretical analysis proves these claims and simulations demonstrate their validity.

The paper is organized as follows. The theoretical derivations of the dynamic model of the P-R-R manipulator are addressed in Section 2. Subsequently, the definition of the synchronization error, design of the A-S controller, and stability analysis of the proposed controller are provided in Section 3. Section 4 shows simulation results. Conclusions are addressed in Section 5.

II. DYNAMIC MODEL

The architecture of the P-R-R manipulator is shown in Figure 1. It consists of following components: a platform; three sets of intermediate links, ball screws and DC brushless motors; three prismatic joints and six revolute joints. The platform with a regular triangular shape corresponds to the end-effector, on which different payloads may be attached. Three intermediate links between the platform and prismatic joints play a role to convert the actuating force into movements of the platform. Both ends of an intermediate link are non-actuated revolute joints. Each prismatic joint moves along a linear guide actuated by an electrical motor via a ball screw mechanism.

Let $\boldsymbol{q} = [\rho_1 \quad \rho_2 \quad \rho_3]^T \in \Re^{3\times 1}$, $\boldsymbol{X_P} = [x_P \quad y_P \quad \alpha]^T \in \Re^{3\times 1}$, $\boldsymbol{X_i} = [x_i \quad y_i \quad \beta_i]^T \in \Re^{3\times 1}$, $i = 1,2,3$. $\boldsymbol{q}$ is the generalized coordinate vector. With respect to the fixed frame, ρ_i, $i = 1,2,3$ denotes the translation of the i^{th} prismatic joints; $\boldsymbol{X_P}$, $\boldsymbol{X_i}$ denote the position and orientation of the platform and the i^{th} intermediate link at their mass centre, respectively. From forward kinematics of the P-R-R manipulator, we derive:

$$\dot{\boldsymbol{q}} = \boldsymbol{J_P} \cdot \dot{\boldsymbol{X}}_{\boldsymbol{P}} \tag{1}$$

$$\dot{\boldsymbol{q}} = \boldsymbol{J}_{\beta_i} \cdot \dot{\boldsymbol{X}}_{\boldsymbol{i}} \qquad i = 1,2,3 \tag{2}$$

where: the Jacobian matrix $\boldsymbol{J_P}$ and $\boldsymbol{J}_{\beta i}$ represent the velocity relationship between the prismatic joints and the platform and the velocity relationship between the i^{th} linkage and platform, respectively. Using the principle of virtual work and following a similar procedure introduced in [7], the dynamic equations of the P-R-R manipulator can be expressed as:

$$\begin{bmatrix} m_P & 0 & 0 \\ 0 & m_P & 0 \\ 0 & 0 & I_P \end{bmatrix} \ddot{\boldsymbol{X}}_{\boldsymbol{P}} + m_s \boldsymbol{J_P^T} \ddot{\boldsymbol{q}} + \sum_{i=1}^{3} \boldsymbol{J}_{\boldsymbol{\beta i}}^{\boldsymbol{T}} \begin{bmatrix} m & 0 & 0 \\ 0 & m & 0 \\ 0 & 0 & I \end{bmatrix} \ddot{\boldsymbol{X}}_{\boldsymbol{i}} + \boldsymbol{J_P^T} \begin{bmatrix} f_{v1} & 0 & 0 \\ 0 & f_{v2} & 0 \\ 0 & 0 & f_{v3} \end{bmatrix} \dot{\boldsymbol{q}} = \boldsymbol{J_P^T F_a} \tag{3}$$

where: m_P, I_P are the mass and the mass moment of inertia of the platform; m, I are the mass and the mass moment of inertia of an intermediate link; m_s is the mass of the prismatic joint; f_{vi}, $i = 1,2,3$ is viscous frictional coefficient; $\boldsymbol{F_a} \in \Re^{3\times 1}$ is the actuating force exerted on the prismatic joints. Since $\ddot{\boldsymbol{X}}_{\boldsymbol{P}}, \ddot{\boldsymbol{X}}_{\boldsymbol{i}}$ are functions of $\boldsymbol{q}, \dot{\boldsymbol{q}}$ and $\ddot{\boldsymbol{q}}$; therefore, (3) can be rewritten into a compact form:

$$\boldsymbol{H}(\boldsymbol{q})\ddot{\boldsymbol{q}} + \boldsymbol{C}(\boldsymbol{q}, \dot{\boldsymbol{q}})\dot{\boldsymbol{q}} = \boldsymbol{F_a} \tag{4}$$

where: $\boldsymbol{H}(\boldsymbol{q}) \in \Re^{3\times 3}$ is the inertia matrix; $\boldsymbol{C}(\boldsymbol{q}, \dot{\boldsymbol{q}})\dot{\boldsymbol{q}} \in \Re^3$ denotes a vector containing the Coriolis, centrifugal, frictional forces and other coupling terms, $\dot{\boldsymbol{H}}(\boldsymbol{q}) - 2\boldsymbol{C}(\boldsymbol{q}, \dot{\boldsymbol{q}})\dot{\boldsymbol{q}}$ is a skew-symmetric matrix [13].

In practice, $\boldsymbol{H}(\boldsymbol{q})$ and $\boldsymbol{C}(\boldsymbol{q}, \dot{\boldsymbol{q}})$ both contain parametric uncertainties mainly due to varying payloads. Define $\boldsymbol{\theta}$ as an m dimensional vector containing the unknown parameters. Using linear parameterization technique, both $\boldsymbol{H}(\boldsymbol{q})$ and $\boldsymbol{C}(\boldsymbol{q}, \dot{\boldsymbol{q}})$ can be expressed linearly in term of unknown parameters listed in $\boldsymbol{\theta}$, as shown in (5):

$$\boldsymbol{H}(\boldsymbol{q})\ddot{\boldsymbol{q}} + \boldsymbol{C}(\boldsymbol{q}, \dot{\boldsymbol{q}})\dot{\boldsymbol{q}} = \boldsymbol{Y}(\boldsymbol{q}, \dot{\boldsymbol{q}}, \ddot{\boldsymbol{q}})\boldsymbol{\theta} \tag{5}$$

where: $\boldsymbol{Y}(\boldsymbol{q}, \dot{\boldsymbol{q}}, \ddot{\boldsymbol{q}}) \in \Re^{3\times m}$ is a regression matrix. Through parameter linearization, we design an adaptation law, which exhibits stable behaviour and guaranteed tracking convergence [12]. Using $\hat{\boldsymbol{\theta}}$ to represent the estimate of $\boldsymbol{\theta}$, an estimated dynamic model is given by:

$$\hat{\boldsymbol{H}}(\boldsymbol{q})\ddot{\boldsymbol{q}} + \hat{\boldsymbol{C}}(\boldsymbol{q}, \dot{\boldsymbol{q}})\dot{\boldsymbol{q}} = \boldsymbol{Y}(\boldsymbol{q}, \dot{\boldsymbol{q}}, \ddot{\boldsymbol{q}})\hat{\boldsymbol{\theta}} \tag{6}$$

where: $\hat{\boldsymbol{H}}(\boldsymbol{q})$, $\hat{\boldsymbol{C}}(\boldsymbol{q}, \dot{\boldsymbol{q}})$ denote the estimate of $\boldsymbol{H}(\boldsymbol{q})$ and $\boldsymbol{C}(\boldsymbol{q}, \dot{\boldsymbol{q}})$, respectively.

III. CONTROLLER DESIGN

A. Synchronization Error

From its mechanical structure, shown in Figure 1, the P-R-R manipulator can be treated as comprised of three constrained sub-manipulators. Each sub-manipulator consists of one intermediate link, one actuated joint (prismatic joint), two non-actuated joints (revolute joints), one ball screw and one DC motor. The end-effector of each

sub-manipulator is the revolute joint connecting the intermediate link and the platform. For each sub-manipulator, the only available feedback information is the position of its prismatic joint, rather than the position of its end-effector; consequently, each sub-manipulator cannot control its end-effector, alone. Therefore, control of the pose of the platform should be achieved by controlling three sub-manipulators, simultaneously, i.e., the motion of each sub-manipulator should coordinate with motions of the other sub-manipulators, which is called synchronization. Considering motion synchronization characteristic of the P-R-R manipulator and inspired by synchronization control for multi-robots, a new error termed synchronization error is defined for the P-R-R manipulator to reduce the pose error of the platform. In order to design the synchronization error, it is necessary to derive a kinematic relationship amongst the positions of all prismatic joints in the sub-manipulators, $\boldsymbol{q}$, and the pose of the P-R-R manipulator end-effector, $\boldsymbol{X_P}$, first. Fortunately, we have already derived it given by (1).

Let $\boldsymbol{X_P^d}$, $\boldsymbol{q^d}$ denotes the desired value of $\boldsymbol{X_P}, \boldsymbol{q}$, respectively. Replacing each term in (1), we obtain:

$$\dot{\boldsymbol{X}}_{\boldsymbol{P}}^{\boldsymbol{d}} = \left(\boldsymbol{J}_{\boldsymbol{P}}^{\boldsymbol{d}}\right)^{-1} \cdot \dot{\boldsymbol{q}}^{\boldsymbol{d}} \tag{7}$$

Left multiplying $\boldsymbol{J}_P^{-1}(t)$ on both sides of (1), subtracting (7), and then left multiplying by $\boldsymbol{J_P}$, the synchronization error is defined as:

$$\boldsymbol{\varepsilon}(t) = \boldsymbol{K_C} \cdot \left(\dot{\boldsymbol{e}}(t) + \boldsymbol{J_P}(t) \cdot \left(\boldsymbol{J}_{\boldsymbol{P}}^{-1}(t) - \left(\boldsymbol{J}_{\boldsymbol{P}}^{\boldsymbol{d}}(t)\right)^{-1} \right) \cdot \dot{\boldsymbol{q}}^{\boldsymbol{d}}(t) \right) \tag{8}$$

where: $\boldsymbol{\varepsilon}(t) \in \Re^{3\times 1}$ is the synchronization error; $\boldsymbol{K_C} \in \Re^{3\times 3}$ is a positive coefficient matrix; $\dot{\boldsymbol{e}}(t) = \left(\dot{\boldsymbol{q}}(t) - \dot{\boldsymbol{q}}^{\boldsymbol{d}}(t)\right) \in \Re^{3\times 1}$ denotes the velocity errors of the three prismatic joints. From (8), it is obvious that each term of $\boldsymbol{\varepsilon}(t)$ contains the actual velocities and desired velocities of the three prismatic joints; therefore, $\boldsymbol{\varepsilon}(t)$ denotes the coordination degree of motions of the three sub-manipulators.

B. A-S Controller Design

In the proposed A-S control algorithm, two types of errors are employed:

Tracking error: $\boldsymbol{e}(t) \in \Re^{3\times 1}$

$$\boldsymbol{e}(t) = \boldsymbol{q}(t) - \boldsymbol{q}^{\boldsymbol{d}}(t) \tag{9}$$

Synchronization error: $\boldsymbol{\varepsilon}(t)$

Then, we define a coupling error, $\boldsymbol{e}^*(t)$, which combines the tracking error and the synchronization error:

$$\boldsymbol{e}^*(t) = \boldsymbol{e}(t) + \boldsymbol{\Gamma} \cdot \boldsymbol{\varepsilon}(t) \tag{10}$$

where: $\boldsymbol{\Gamma} \in \Re^{3\times 3}$ is a positive constant coefficient matrix.

Define a vector $\boldsymbol{u}(t) \in \Re^{3\times 1}$, similarly as defined in [9]:

$$\boldsymbol{u}(t) = \dot{\boldsymbol{q}}^{\boldsymbol{d}}(t) - \boldsymbol{\Gamma}\dot{\boldsymbol{\varepsilon}}(t) - \boldsymbol{\Lambda}\boldsymbol{e}^*(t) \tag{11}$$

where: $\boldsymbol{\Lambda} \in \Re^{3\times 3}$ is a symmetric positive definite matrix. The vector $\boldsymbol{u}(t)$ formed by modifying the desired velocity $\dot{\boldsymbol{q}}^{\boldsymbol{d}}$ using the coupling error $\boldsymbol{e}^*(t)$ and the derivative of the synchronization error, may be called "reference velocity". The introduction of $\boldsymbol{u}(t)$ guarantees the convergence of the tracking error and the synchronization error [12]. Define another vector $\boldsymbol{r}(t) \in \Re^{3\times 1}$, which can be treated as a measure of tracking accuracy:

$$\begin{aligned} \boldsymbol{r}(t) &= \dot{\boldsymbol{q}}(t) - \boldsymbol{u}(t) = \dot{\boldsymbol{q}}(t) - \dot{\boldsymbol{q}}^{\boldsymbol{d}}(t) + \boldsymbol{\Gamma}\dot{\boldsymbol{\varepsilon}}(t) + \boldsymbol{\Lambda}\boldsymbol{e}^*(t) \\ &= \dot{\boldsymbol{e}}^*(t) + \boldsymbol{\Lambda}\boldsymbol{e}^*(t) \end{aligned} \tag{12}$$

Our objective is to design a control law such that the coupling error, i.e., the position error, velocity error, and synchronization errors, all converge to zero. In other words, the control law should be able to restrict $\boldsymbol{r}(t)$ to lie on the sliding surface:

$$\boldsymbol{r}(t) = \dot{\boldsymbol{e}}^*(t) + \boldsymbol{\Lambda}\boldsymbol{e}^*(t) = 0 \tag{13}$$

The control law and adaptation law are defined as follows:

Control law:

$$\boldsymbol{F_a} = \hat{\boldsymbol{H}}(\boldsymbol{q})\dot{\boldsymbol{u}} + \hat{\boldsymbol{C}}(\boldsymbol{q},\dot{\boldsymbol{q}})\boldsymbol{u} - \boldsymbol{K_r}\boldsymbol{r}(t) - \boldsymbol{K_e}\boldsymbol{e}^*(t) \tag{14}$$

where: $\boldsymbol{K_r} \in \Re^{3\times 3}, \boldsymbol{K_e} \in \Re^{3\times 3}$ are both positive diagonal gain matrices. In a similar manner to the derivation of (5), we have:

$$\boldsymbol{F_a} = \boldsymbol{Y}(\boldsymbol{q},\dot{\boldsymbol{q}},\boldsymbol{u},\dot{\boldsymbol{u}})\hat{\boldsymbol{\theta}} - \boldsymbol{K_r}\boldsymbol{r}(t) - \boldsymbol{K_e}\boldsymbol{e}^*(t) \tag{15}$$

Adaptation law:

$$\dot{\hat{\boldsymbol{\theta}}}(t) = -\boldsymbol{P}(t)\boldsymbol{Y}(\boldsymbol{q},\dot{\boldsymbol{q}},\boldsymbol{u},\dot{\boldsymbol{u}})^T(\boldsymbol{r}(t) + \boldsymbol{Y}(\boldsymbol{q},\dot{\boldsymbol{q}},\boldsymbol{u},\dot{\boldsymbol{u}})\tilde{\boldsymbol{\theta}}) \tag{16}$$

$$d(\boldsymbol{P}^{-1})/dt = -\lambda(t)\boldsymbol{P}^{-1}(t) + \boldsymbol{Y}(\boldsymbol{q},\dot{\boldsymbol{q}},\boldsymbol{u},\dot{\boldsymbol{u}})^T\boldsymbol{Y}(\boldsymbol{q},\dot{\boldsymbol{q}},\boldsymbol{u},\dot{\boldsymbol{u}}) \tag{17}$$

$$\lambda(t) = \lambda_0(1 - \|\boldsymbol{P}\|/k_0) \tag{18}$$

where: $\boldsymbol{P}(t) \in \Re^{3\times 3}$ is gain matrix of the estimator; $\tilde{\boldsymbol{\theta}}(t) = \hat{\boldsymbol{\theta}}(t) - \boldsymbol{\theta}(t)$; λ_0, k_0 are positive constants representing the maximum forgetting rate and a pre-specified bound for the magnitude of $\boldsymbol{P}(t)$. This is actually a Bounded-Gain-Forgetting (BGF) estimator, which can filter noise and small disturbances, and avoid oscillation of the estimated parameters [12].

C. Stability Analysis

Substituting the control law (14) into the dynamic equations (4), the closed-loop dynamics of the P-R-R manipulator are derived as:

$$\begin{aligned}&\boldsymbol{H}(\boldsymbol{q})\ddot{\boldsymbol{q}}+\boldsymbol{C}(\boldsymbol{q},\dot{\boldsymbol{q}})\dot{\boldsymbol{q}}=\hat{\boldsymbol{H}}(\boldsymbol{q})\dot{\boldsymbol{u}}+\hat{\boldsymbol{C}}(\boldsymbol{q},\dot{\boldsymbol{q}})\boldsymbol{u}-\boldsymbol{K}_r\boldsymbol{r}(t)-\boldsymbol{K}_e\boldsymbol{e}^*(t)\\&\Rightarrow\boldsymbol{H}(\boldsymbol{q})\dot{\boldsymbol{r}}(t)+\boldsymbol{C}(\boldsymbol{q},\dot{\boldsymbol{q}})\boldsymbol{r}(t)+\boldsymbol{K}_r\boldsymbol{r}(t)+\boldsymbol{K}_e\boldsymbol{e}^*(t)\\&\quad=\boldsymbol{Y}(\boldsymbol{q},\dot{\boldsymbol{q}},\boldsymbol{u},\dot{\boldsymbol{u}})\tilde{\boldsymbol{\theta}}\end{aligned}\tag{19}$$

Through construction of a Lyapunov function and use of Barbalat's lemma [12], the proposed Theorem 1 and Theorem 2, which address the stability of the proposed control algorithm, are proved.

Theorem 1: For the proposed control algorithm, if the desired trajectories are continuous and bounded, then $\boldsymbol{e}(t)$ and $\dot{\boldsymbol{e}}(t)$ are both bounded.

Proof: Define a positive definite function as:

$$V(t)=\frac{1}{2}[\boldsymbol{r}^T(t)\boldsymbol{H}(\boldsymbol{q})\boldsymbol{r}(t)+\tilde{\boldsymbol{\theta}}^T(t)\boldsymbol{P}(t)^{-1}\tilde{\boldsymbol{\theta}}(t)+\boldsymbol{e}^*(t)^T\boldsymbol{K}_e\boldsymbol{e}^*(t)]\tag{20}$$

Differentiating $V(t)$ with respect to time yields:

$$\begin{aligned}\dot{V}(t)&=\boldsymbol{r}^T(t)\boldsymbol{H}(\boldsymbol{q})\dot{\boldsymbol{r}}(t)+\frac{1}{2}\boldsymbol{r}^T(t)\dot{\boldsymbol{H}}(\boldsymbol{q})\boldsymbol{r}(t)+\tilde{\boldsymbol{\theta}}^T(t)\boldsymbol{P}(t)^{-1}\dot{\tilde{\boldsymbol{\theta}}}(t)\\&\quad+\frac{1}{2}\tilde{\boldsymbol{\theta}}^T(t)\frac{d}{dt}(\boldsymbol{P}(t)^{-1})\tilde{\boldsymbol{\theta}}(t)+\boldsymbol{e}^*(t)^T\boldsymbol{K}_e\dot{\boldsymbol{e}}^*(t)\end{aligned}\tag{21}$$

Left multiplying both sides of (19) by $\boldsymbol{r}^T$, then substituting into (21), and utilizing (13), (16), (17), we have

$$\begin{aligned}\dot{V}(t)&=-\boldsymbol{r}^T(t)\boldsymbol{K}_r\boldsymbol{r}(t)-(\dot{\boldsymbol{e}}^*(t)^T+\boldsymbol{e}^*(t)^T\boldsymbol{\Lambda})\boldsymbol{K}_e\boldsymbol{e}^*(t)\\&\quad-\frac{1}{2}\tilde{\boldsymbol{\theta}}^T(t)\boldsymbol{Y}^T\boldsymbol{Y}\tilde{\boldsymbol{\theta}}(t)-\frac{\lambda(t)}{2}\tilde{\boldsymbol{\theta}}^T(t)\boldsymbol{P}(t)^{-1}\tilde{\boldsymbol{\theta}}(t)+\boldsymbol{e}^*(t)^T\boldsymbol{K}_e\dot{\boldsymbol{e}}^*(t)\\&=-\boldsymbol{r}^T(t)\boldsymbol{K}_r\boldsymbol{r}(t)-\boldsymbol{e}^*(t)^T\boldsymbol{\Lambda}\boldsymbol{K}_e\boldsymbol{e}^*(t)-\frac{1}{2}\tilde{\boldsymbol{\theta}}^T(t)\boldsymbol{Y}^T\boldsymbol{Y}\tilde{\boldsymbol{\theta}}(t)\\&\quad-\frac{\lambda(t)}{2}\tilde{\boldsymbol{\theta}}^T(t)\boldsymbol{P}(t)^{-1}\tilde{\boldsymbol{\theta}}(t)\\&\le 0\end{aligned}\tag{22}$$

Differentiating $\dot{V}(t)$ with respect to time yields

$$\begin{aligned}\ddot{V}(t)&=-2\boldsymbol{r}^T(t)\boldsymbol{K}_r\dot{\boldsymbol{r}}(t)-2\boldsymbol{e}^*(t)^T\boldsymbol{\Lambda}\boldsymbol{K}_e\dot{\boldsymbol{e}}^*(t)\\&\quad-\tilde{\boldsymbol{\theta}}^T(t)\boldsymbol{Y}^T\boldsymbol{Y}\dot{\tilde{\boldsymbol{\theta}}}(t)-\tilde{\boldsymbol{\theta}}^T(t)\boldsymbol{Y}^T\dot{\boldsymbol{Y}}\tilde{\boldsymbol{\theta}}(t)\\&\quad-\frac{\dot{\lambda}(t)}{2}\tilde{\boldsymbol{\theta}}^T(t)\boldsymbol{P}(t)^{-1}\tilde{\boldsymbol{\theta}}(t)-\frac{3\lambda(t)}{2}\tilde{\boldsymbol{\theta}}^T(t)\boldsymbol{Y}^T\boldsymbol{Y}\tilde{\boldsymbol{\theta}}(t)\\&\quad+\frac{\lambda(t)^2}{2}\tilde{\boldsymbol{\theta}}^T(t)\boldsymbol{P}(t)^{-1}\tilde{\boldsymbol{\theta}}(t)\end{aligned}\tag{23}$$

Since $\dot{V}(t)\le 0$, hence $\boldsymbol{r}(t)$, $\boldsymbol{e}^*(t)$ and $\tilde{\boldsymbol{\theta}}(t)$ are bounded. From (13), $\dot{\boldsymbol{e}}^*(t)$ is bounded. On the other hand, from (19), $\dot{\boldsymbol{r}}(t)$ is bounded. Since the manipulator has a bounded workspace, in which if the desired trajectory is continuous and bounded, then $\boldsymbol{q}^{\boldsymbol{d}}(t)$, $\dot{\boldsymbol{q}}^{\boldsymbol{d}}(t)$ and $\ddot{\boldsymbol{q}}^{\boldsymbol{d}}(t)$ are all bounded. Since $\boldsymbol{e}^*(t)$ is bounded, $\boldsymbol{J}_{\boldsymbol{P}}^{\boldsymbol{d}}(t)$ and $\dot{\boldsymbol{q}}^{\boldsymbol{d}}(t)$ are bounded, substituting (8) into (10), we can derive:

$$\boldsymbol{e}(t)+\boldsymbol{K}_{\boldsymbol{B}}\dot{\boldsymbol{e}}(t)=\boldsymbol{w}\tag{24}$$

where: $\boldsymbol{K}_{\boldsymbol{B}}=\boldsymbol{\Gamma}\boldsymbol{K}_{\boldsymbol{C}}\in\Re^{3\times 3}$ is a positive constant matrix, $\boldsymbol{w}\in\Re^3$ is a bounded vector. Then it is easy to prove that $\boldsymbol{e}(t)$ and $\dot{\boldsymbol{e}}(t)$ are both bounded. Therefore, as a conclusion, $\boldsymbol{e}(t)$ and $\dot{\boldsymbol{e}}(t)$ are both bounded. □

Theorem 2: If the desired trajectories are continuous and bounded, and Y is persistently exciting, then the proposed controller gives rise to asymptotic convergence of tracking error, synchronization error, coupling error and unknown quantity estimated errors, i.e., $\boldsymbol{e}(t)\to 0$, $\boldsymbol{\varepsilon}(t)\to 0$, $\boldsymbol{e}^*(t)\to 0$ and $\tilde{\boldsymbol{\theta}}(t)\to 0$ as $t\to\infty$.

Proof: Since the desired trajectory of the platform in bounded and continuous, $\boldsymbol{Y}$ is also bounded and continuous; subsequently, $\dot{\boldsymbol{Y}}$ is bounded. When $\boldsymbol{Y}$ is persistently exciting, then $\boldsymbol{P}(t)^{-1}$ and $\lambda(t)$ are both bounded [12]. Hence, from (23), $\ddot{V}(t)$ is bounded. Since the differentiable function $V(t)$ is bounded and $\ddot{V}(t)$ is bounded, from Barbalat's lemma, it follows that $\dot{V}(t)\to 0$ as time $t\to\infty$. From (22), it is obvious that $\boldsymbol{r}(t)\to 0$, $\boldsymbol{e}^*(t)\to 0$, and $\tilde{\boldsymbol{\theta}}(t)\to 0$ as $t\to\infty$. Since $\dot{\boldsymbol{r}}(t)$ and $\dot{\boldsymbol{e}}^*(t)$ are bounded, as derived in Theorem 1, from (10) and (12), we can derive that $\ddot{\boldsymbol{e}}(t)$ is bounded. Similarly, from Barbalat's lemma, we can derive that $\dot{\boldsymbol{e}}(t)\to 0$ as $t\to\infty$. Finally, since $\dot{\boldsymbol{e}}(t)\to 0$ and $\boldsymbol{e}^*(t)\to 0$ as $t\to\infty$, from (8) and (10), we can derive that $\boldsymbol{e}(t)\to 0, \boldsymbol{\varepsilon}(t)\to 0$ as $t\to\infty$. □

IV. SIMULATION

In order to verify the above claims outlined in Theorem 1 and 2, and verify the effect of the synchronization error on trajectory tracking, simulations of the A-S controller employed on the P-R-R manipulator have been accomplished. During simulations, it is assumed that we have already known the exact values of all system parameters obtained from theoretical calculations. These values are listed in Table 1. For simplicity, without loss of generality, we set the initial pose of the platform as: $x_I=0.0mm$, $y_I=0.0mm$, $\phi_I=10\deg$ and set the final pose of the platform as: $x_f=20.0mm$, $y_f=10.0mm$, $\phi_f=60\deg$, corresponding to the fixed frame, where x,y is the position of the mass center of the platform, ϕ is the rotation angle. The desired trajectory between these two pose is three sinusoidal wave functions with smooth accelerations and decelerations as follows:

$$\begin{cases}x_P=x_I+\dfrac{x_f}{t_f}t-\dfrac{x_f}{2\pi}\cdot\sin\left(\dfrac{2\pi}{t_f}t\right)\\ y_P=y_I+\dfrac{y_f}{t_f}t-\dfrac{y_f}{2\pi}\cdot\sin\left(\dfrac{2\pi}{t_f}t\right)\\ \phi_P=\dfrac{\phi_I\cdot\pi}{180}+\dfrac{\phi_f\cdot\pi}{t_f\cdot 180}t-\dfrac{\phi_f}{360}\cdot\sin\left(\dfrac{2\pi}{t_f}t\right)\end{cases}\tag{25}$$

where: $t_f = 20ms$. Hence, $v_x = 1m/s, v_y = 0.5m/s, v_\phi = 43.63rad/s$. Through trials, $\boldsymbol{K_r} = diag\{18\}, \boldsymbol{K_e} = diag\{50.4\}, \boldsymbol{\Gamma} = diag\{1.03\}$, $\boldsymbol{\Lambda} = diag\{0.04\}$ of the A-S controller have been found to achieve the best accuracy.

We use MATLAB to perform the simulations. Figure 2 illustrates the actual and desired pose profiles of the platform using the A-S controller. Three graphs illustrate the profile of x position, y position, and rotation angle ϕ of the platform, in order. In each graph, the dashed line represents the desired profile, and the solid line represents the actual profile. Figure 3 illustrates the pose error profiles of the platform using the A-S controller. Three graphs illustrate the error profile of x position, y position, and rotation angle ϕ of the platform, respectively. Figure 4 illustrates the torque profiles of the three DC motors using the A-S controller. From Figure 3 and Figure 4, the maximum errors of x position, y position, rotation angle ϕ of the platform, and the maximum torque of the three DC motors employing the A-S controller are listed in Table 2. Analyzing data listed in Table 2, it is obvious that A-S control achieves excellent trajectory tracking performance.

V. CONCLUSION

A new adaptive synchronization control algorithm is proposed for trajectory control of a P-R-R type planar parallel manipulator, which is developed for assembling tasks. The proposed A-S controller is designed by incorporating synchronization control into the adaptive control structure. Since the P-R-R manipulator can be treated as comprised of three constrained sub-manipulators, through controlling motions of all sub-manipulators synchronously and employing synchronization error, the pose error of the platform of the manipulator is reduced during trajectory tracking. It has been theoretically proved that the A-S controller guarantees asymptotic convergence to zero of tracking errors and synchronization error if the regression matrix is persistently exciting. The condition, under which the regression matrix is persistently exciting, will be studied in the future research. Analyzing simulation results, it is demonstrated that the proposed controller can achieve pretty good trajectory tracking performance.

REFERENCES

[1] J. A. Carretero, R. P. Podhorodeski, M. A. Nahon, and C. M. Gosselin, "Kinematic analysis and optimization of a new three degree-of-freedom spatial parallel manipulator", *J. Mechanical Design*, Vol. 122, No. 1, pp. 17-24, 2000.

[2] G. R. Dunlop, and T. P. Jones, "Position analysis of a 3-DOF parallel manipulator", *Mechanism and Machine Theory*, Vol. 32, No. 8, pp. 903-920, 1997.

[3] F. Pierrot, P. Dauchez, and A. Fournier, "Towards a fully parallel 6 d.o.f. robot for high speed applications", *Proc. IEEE Conf. Robotics and Automation*, pp. 1288-1293, Sacramento, California, 1991.

[4] M. Honegger, R. Brega and G. Schweitzer, "Application of a nonlinear adaptive controller to a 6 dof parallel manipulator", *Proc. IEEE Conf. Robotics and Automation*, pp.1930-1935, San Francisco, 2000.

[5] K. Ryo, H. Tsutomu and Y. Kan, "The sway compensation trajectory for a biped robot", *Proc. IEEE Conf. Robotics and Automation*, pp. 925-931, Taipei, Taiwan, 2003.

[6] B. Kang, and J. K. Mills, "Dynamic modeling and vibration control of high speed planar parallel manipulator", *Proc. of IEEE Conf. Intelligent Robots and Systems*, pp. 1287-1292, Maui, Hawaii, USA, Oct. 2001.

[7] B. Kang, J. Chu, and J. K. Mills, "Design of high speed planar parallel manipulator and multiple simultaneous specification control', *Proc. IEEE Conf. Robotics and Automation*, pp. 2723-2728, Seoul, Korea, May 2001.

[8] E. Kemalettin, K. Okyay, and S. Asif, "Robust control of a direct drive manipulator", *Proc. IEEE Int. Symposium, Intelligent Control*, pp. 108-113, Piscataway, NJ, USA, 1998.

[9] J. –J. E. Slotine, and W. Li, "Adaptive manipulator control: a case study", *IEEE Trans. Automatic Control*, Vol. 33, No. 11, pp. 995-1003, Nov. 1988.

[10] P. Chen, K. Zhou, and A. Ogilive, "Development of a neural network module for improving the performance of a commercial robot", *Proc. World Automation Conf.,* pp. 146-154, Alaska, USA, 1998.

[11] D. Sun, and J. K. Mills, " Adaptive synchronization control for coordination of multi-robot assembly tasks", *IEEE Trans. Robot. Automat*., Vol. 18, No. 4, pp. 498-510, Aug. 2002.

[12] J. –J. E. Slotine, and W. P. Li, Applied nonlinear control, Englewood Cliffs, N.J.: Prentice Hall, 1991.

[13] S. Li, Z. Feng, and H. Fang, "Variable structure control for 6-6 parallel manipulators based on cascaded CMAC", *Proc. 4th World Cong. Intelligent Control and Automations*, pp. 1939-1943, Shanghai, P.R. China, June 2002.

TABLE 1. PARAMETERS FOR SIMULATIONS

Items	Values
Side length of the platform	$100mm$
Length of the intermediate link	$200mm$
Lead of the ball screw	$6mm$
Mass of the platform	$2.5kg$
Mass of the intermediate link	$0.2kg$
Mass of the prismatic joint	$0.2kg$
Mass inertia of the motor	$2.0e-5kg \cdot m^2$
Viscous frictional coefficient	$1.3e-4kg/s$

TABLE 2. SIMULATION RESULTS

Items	Values
Maximum X position error	$-0.210mm$
Maximum Y position error	$-0.083mm$
Maximum rotation angle error	-0.324 deg
Maximum torque	$8.532Nm$

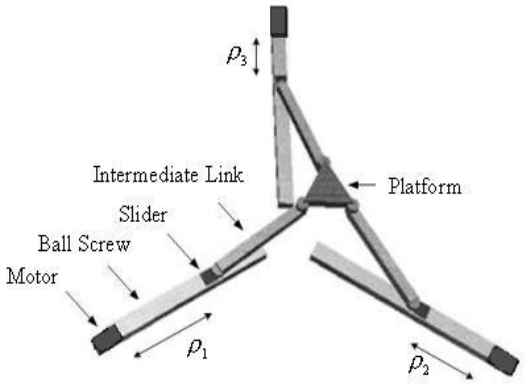

Figure 1. Architecture of the P-R-R manipulator

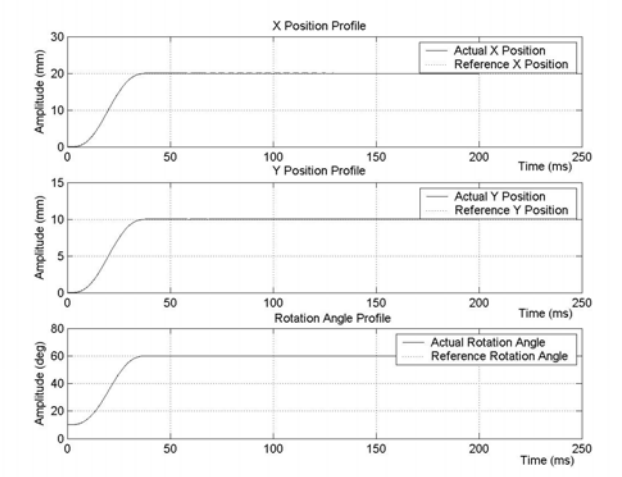

Figure 2. Pose profile of the platform using the A-S controller

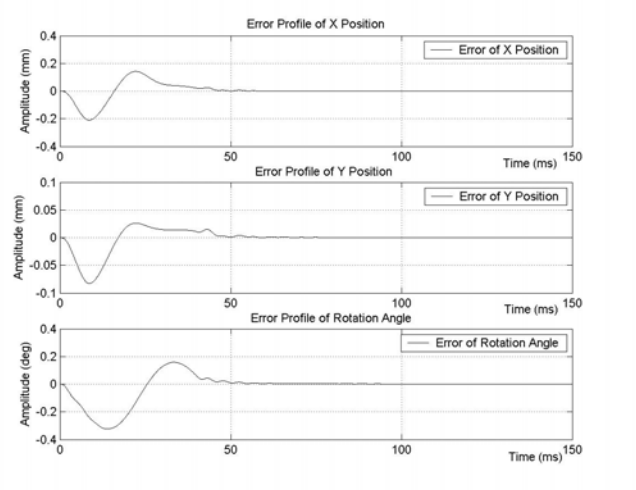

Figure 3. Pose error profiles of the platform using the A-S controller

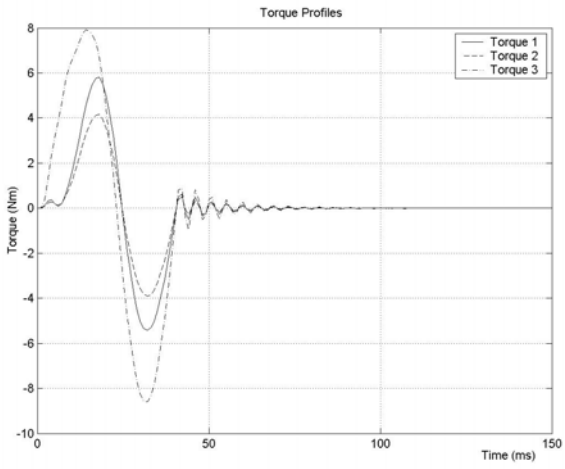

Figure 4. Torque profiles of the three DC motors using the A-S controller